Acta Oceanol. Sin., 2012, Vol. 31, No. 5, P. 1-10
DOI: 10.1007/s13131-012-0231-y
http://www.hyxb.org.cn
E-mail: hyxbe@263.net

A review on the South China Sea western boundary current

FANG Guohong[1], WANG Gang[1,2*], FANG Yue[3], FANG Wendong[4]

[1] Key Laboratory of Marine Science and Numerical Modeling, First Institute of Oceanography, State Oceanic Administration, Qingdao 266061, China

[2] Key Laboratory of Data Analysis and Applications, First Institute of Oceanography, State Oceanic Administration, Qingdao 266061, China

[3] Center for Ocean and Climate Research, First Institute of Oceanography, State Oceanic Administration, Qingdao 266061, China

[4] State Key Laboratory of Tropical Oceanography, South China Sea Institute of Oceanology, Chinese Academy of Sciences, Guangzhou 510301, China

Received 12 March 2012; accepted 3 July 2012

Abstract
The advances in understanding the South China Sea (SCS) western boundary current (SCSwbc) have been reviewed since the works of Dale (1956) and Wyrtki (1961) in the middle of the 20th century. The features of the pattern of SCSwbc and the oceanic phenomena associated with it are focused on. The current is driven mainly by monsoon over the SCS and partially by winds over the tropical Pacific governed by the island rule. The SCSwbc exhibits strong seasonal variation in its direction and patterns. In winter, the current is strong and flows southwestward along the South China shelf and slope from the east of Dongsha Islands to the northern central Vietnamese coast, then turns to the south along the central and southern Vietnamese coast, and finally partially exits the SCS through the Karimata Strait. In summer and early fall, the SCSwbc can be divided into three segments based on their characteristics. The southern segment is stable, flowing northward from the Karimata Strait up to about 11°N, where it separates from the coast forming an eastward offshore current. The separation of the current from Vietnamese coast induces some striking features, such as upwelling and cold sea-surface temperature. The middle segment off the central Vietnamese coast may have a bimodal behavior: northward coastal current and meandering current in early summer (June–July), and cyclonic gyre in later summer and early fall (August–September). The northern segment is featured by the summer SCS Warm Current on the South China shelf and a southwestward subsurface current along the continental slope.

Key words: South China Sea, western boundary current, Vietnam offshore current, upwelling, subsurface current

1 Introduction

As one of the largest marginal seas in the world, with an area of about 3.5×10^6 km^2, the South China Sea (SCS) is featured by a strong current along its western boundary, called the South China Sea western boundary current (SCSwbc). The western boundary current is very similar to those in the great open oceans such as the Pacific and Atlantic Oceans. In contrast to the circulation in the great open oceans, however, the SCSwbc is seasonally reversible. In the middle of the last century, Dale (1956) deduced it from drift current data, which might be the first record on this current (Fig. 1). In the monthly schematic surface current charts of the SCS he presented, the westward intensification can be clearly observed. Based on 50 a historical data collected in the Southeast Asian seas, Wyrtki (1961) gave a general description of the bimonthly current of the SCS, including the formation, evolution and decay of the SCSwbc. Figure 2 is the surface current diagram for February and August given by Wyrtki (1961). In history, there have been

Foundation item: The National Basic Research Program ("973" Program) of China under contract Nos 2011CB403500 and 2012CB957803; the National Natural Science Foundation of China under contract Nos 41006018 and 40730842; and the National High Technology Research and Development Program ("863" Program) of China under contract No. 2008AA09A402.
*Corresponding author, E-mail: wangg@fio.org.cn

different names for the SCSwbc: monsoon current along the coast of Vietnam (Wyrtki, 1961), coastal jet off Vietnam (Shaw and Chao, 1994; Chu et al., 1998), alongshore current off Vietnam (Shaw and Chao, 1994), western boundary current (along/off the Chinese and Vietnamese coasts) (Metzger and Hurlburt, 1996; Shaw et al., 1998; Fang and Fang, 1998; Takano et al., 1998; Tangang et al., 2011), Vietnam coastal jet/current (Chu et al., 1998; Cai et al., 2007), and South China Sea monsoon jet (Li et al., 2000).

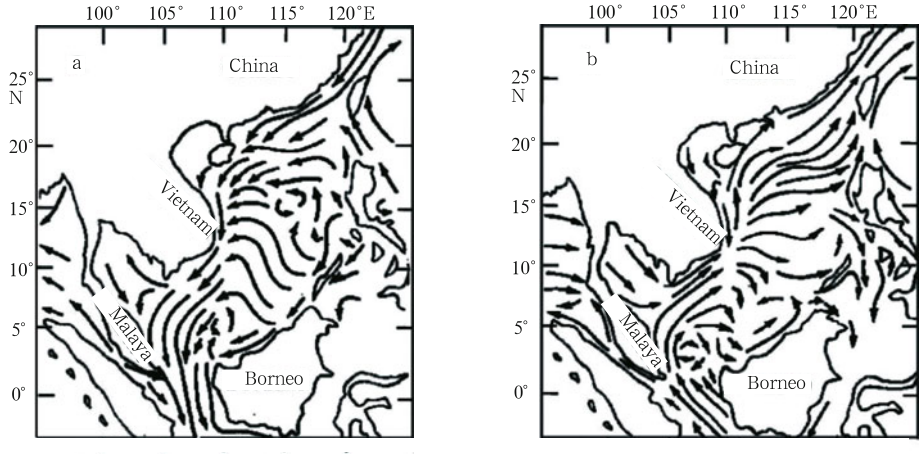

Fig.1. Surface currents of the South China Sea by Dale (1956). a. January and b. July. The westward intensification along the Vietnamese coast can be clearly observed.

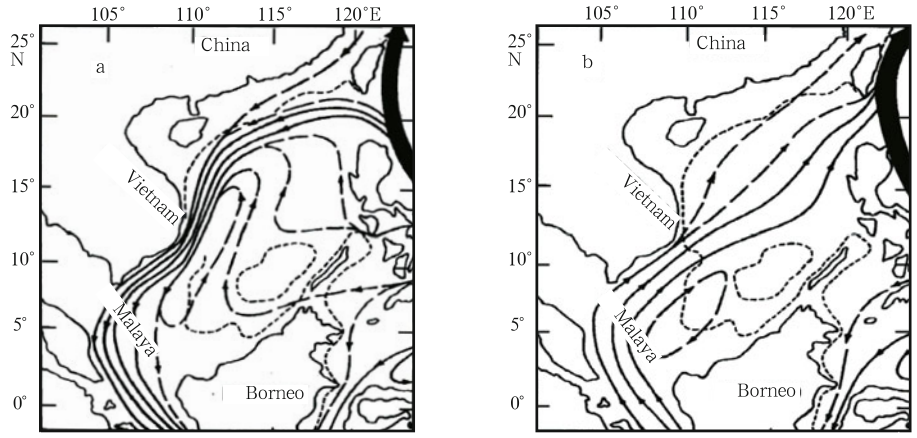

Fig.2. Surface circulation pattern drawn by Wyrtki (1961). a. February and b. August.

The SCSwbc is a main contributor for the redistribution of water properties, momentum, energy and nutrients in the SCS. The current is mainly wind-driven and thus has a clear annual cycle corresponding to monsoon transition(Liu et al., 2001), and it in turn plays a key role in the seasonal reversal of the upper-layer current of the SCS (Hu et al., 2000; Du et al., 2004; Zhou et al., 2010) and significantly influences the regional climate (e. g., Xie et al., 2003).

Owing to its important role in the SCS circulation, the SCSwbc has been attracting much attention in the last 30 a. Some details on the feature of SCSwbc have been revealed through in situ observations, floats, satellites data, and numerical simulations. However, the in situ observations in relation with the SCSwbc can only be found in a limited number of literatures (e. g., Qiu et al., 1984; Guo et al., 1985; Huang et al., 1997; Fang et al., 1998; Penjan et al., 2001; Fang et al., 2002; Du et al., 2004; Dippner et al., 2007; Chen et al., 2010; Fang et al., 2010). The in situ observations have been and will still be crucial sources for revealing new features and verifying the proposed features of the current, though the observations so far conducted only provided data in limited areas and time spans.

The most widely used data for the analysis of the SCSwbc are sea surface height (SSH) from

TOPEX/Posidon(T/P) altimetry(Shaw et al., 1998; Ho et al., 2000; Wang et al., 2000; Xie et al., 2003; Bao et al., 2005; Wang, Wang et al., 2006; Rong et al., 2007; Cai and He, 2010). These data are sometimes analyzed with the method of empirical orthogonal function (EOF) to figure out the temporal and spatial patterns of surface SCSwbc. Argo floats passing through this region are also helpful to reveal the characteristics of SCSwbc (He and Sui, 2010; Zhou et al., 2010), but the data are sparse.

A numerical simulation is another widely used approach to study the SCSwbc. The models are mostly primitive equation models (e. g., Shaw and Chao, 1994; Chao et al., 1995; Chao et al., 1996; Metzger and Hurlburt, 1996; Chu et al., 1998; Shaw et al., 1998; Takano et al., 1998; Chu et al., 1999; Chern and Wang, 2003; Qu et al., 2004; Fang et al., 2005; Wang, Fang et al., 2006; Fang et al., 2009; Tangang et al., 2011). Idealized and simplified models are usually designed to study the mechanism of the current for some particular cases (e. g., Li et al., 1994; Fang et al., 1996; Chao et al., 2006; Wang ,Chen et al., 2006; Cai et al., 2007).

2 Features of SCSwbc in winter

Since the SCSwbc is mainly driven by winds, it shows obvious seasonal transition following the reversal of SCS monsoon. To obtain a clear picture of the pattern of SCSwbc, we will focus on the current patterns in winter and summer, respectively, as the SCS monsoon is strong in winter and summer.

Wyrtki (1961) illustrated the pattern of SCSwbc every 2 months based on ship drift data. The winter circulation can be represented by his February diagram shown in Fig. 2a. It can be seen that the winter SCSwbc mainly originates from the Luzon Strait and runs straightforward toward the Karimata Strait. The interior circulation may enhance the current to some extent.

Based on the hydrographic observations in January and December 1981 and January and February 1982, Guo et al. (1985) found a strong southwest current, and named it the SCS Branch of the Kuroshio. Fang et al. (2005) extended the concept of the SCS Branch of the Kuroshio to the SCS Branch of the Pacific-to-Indian Ocean throughflow in view that the current continues to flow along the western boundary and exit the SCS toward the Indian Ocean. They further suggested that the southwestward current observed by Guo et al. (1985) should be a combination of the SCS Branch of the Pacific-to-Indian Ocean throughflow with the interior circulation gyre located in the northern SCS deep basin, which was named Luzon gyre by Fang et al. (2009). In fact, the winter SCSwbc consists of two components: the western boundary current of the interior circulation and the SCS Branch of the Pacific-to-Indian Ocean throughflow.

More complete structure was revealed in the 1990s in a number of numerical models (Li et al., 1994; Shaw and Chao, 1994; Fang et al., 1996; Metzger and Hurlburt, 1996). Fang et al. (1998) summarized observational and model results, and presented refined schematic diagrams for winter and summer circulation as shown in Fig. 3. Shaw et al. (1998) and Li et al. (2000) used the sea-surface height anomalies (SSHA) observed by a satellite altimeter to infer the SCS circulation. Figure 4 is a climatological mean

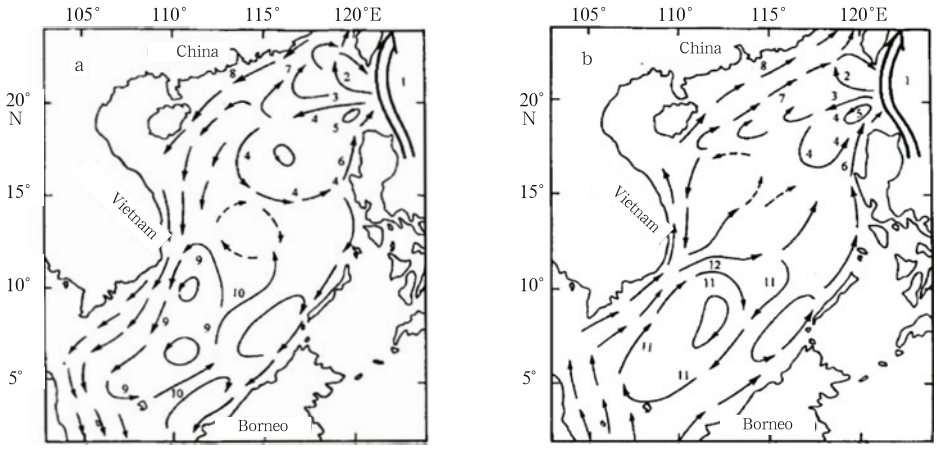

Fig.3. Schematic diagram for the SCS upper layer general circulation by Fang et al. (1998). a. winter and b. summer.

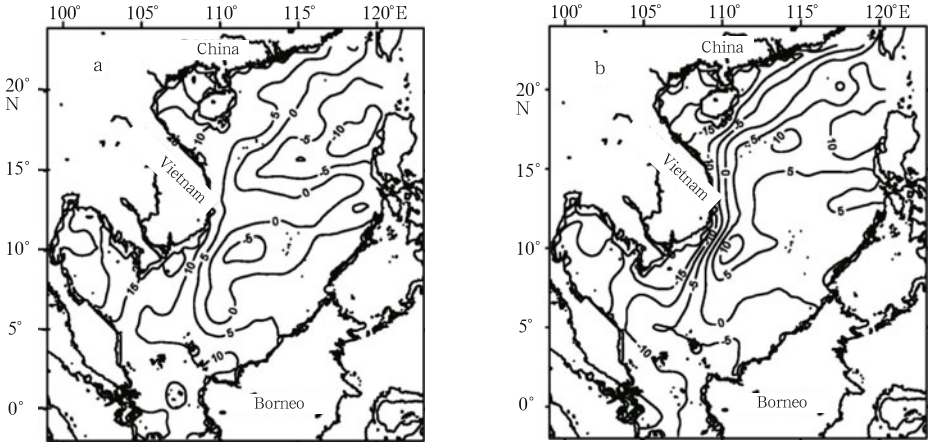

Fig.4. Climatological mean sea-surface height anomaly (SSHA) during 1993–2003 by Fang et al. (2006). a. January and b. July. The anomalous upper layer geostrophic current in off-equatorial is parallel to the contours of SSHA with higher height on their right side.

SSHA plot for only January and July (the other months are not shown). The monthly SSHA diagrams show that the winter SCSwbc develops in middle fall (October), and terminates in early spring (March) of the following year. The mature period is from November to February next year, when it runs southwestward along the South China continental shelf and slope and turns southward along the Vietnamese coast. On arriving the Sunda shelf, one part of it continues to flow towards the Java Sea through the Karimata Strait, where the throughflow volume transport can reach 3.6×10^6 m^3/s (Fang et al., 2010), and the other part turns eastward and forms a cyclonic gyre (Fig. 3).

Observational evidence for deep SCSwbc in winter is very limited. The dynamic calculation based on the hydrographic observation by Guo et al. (1985, their Fig. 6) shows that the southwestward current near the South China continental slope can extend to a depth of about 800 m.

3 Features of SCSwbc in summer

The SCSwbc in summer is generally much weaker than in winter, but its structure and evolution are much more complicated. The northward western boundary current begins in May appearing as a simple northward current. From June it can be roughly divided into three segments. The southern segment is from the Karimata Strait to the turning point of the Vietnamese coastline at about 11°N. This segment of the flow is relative strong and stable, thus can be well recognized. The middle segment is from the turning point of the Vietnamese coastline to the mouth of the Beibu Gulf. This segment of flow is weak and variable. The northern segment is on/along the South China shelf and continental slope. There seems no doubt about the surface flow, while the subsurface flow needs further clarification. The following are some most distinguished features.

3.1 *Vietnam offshore Current*

As mentioned above, the southern segment of the summer SCSwbc is relative strong and stable. It starts from the Karimata Strait and flows northward along the southern Malay Peninsula, then passes by the mouth of Gulf of Thailand and flows along the southeastern Vietnamese coast. When this boundary current reaches the area at 11°N, it turns to the east forming an offshore current. This offshore nature can be seen in Dale's and Wyrtki's diagrams (Figs 1b and 2b). This feature was first revealed by the hydrographic observations by Fang et al. (1998) [also see Fang et al. (2002)]. The offshore current was named the Southeast Vietnam Offshore Current by Fang et al. (1998, Fig. 3b). In this review we call it the Vietnam Offshore Current (VOC) for short.

The VOC was verified with the satellite observations by Ho et al. (2000). T/P altimeter measurements from December 1992 to April 1998 show that a high-variability area of the SSH exists off the central Vietnam coast (12°–13°N, 110°–112°E). The EOF analysis shows that it has the highest SSH in February and the lowest SSH in August.

Almost all numerical models can reproduce the

VOC. The position of the VOC's separation from coast, however, varies between 10° and 14°N (Li et al., 1994; Shaw and Chao, 1994; Chao et al., 1996; Fang et al., 1996; Chu et al., 1998; Fang, Fang et al., 1998; 1998; Fang, Guo et al., 1998; Fang and Fang, 1998; Takano et al., 1998). Shaw and Chao (1994) believed it was caused by the turning of the orientation of the Vietnamese coastline. Takano et al. (1998) suggested that the wind stress curl distribution played an important role for the separation. Shaw et al. (1998) further found that the VOC separates from the Vietnamese coast along exactly the line of zero curl of wind stress. The separation and its position have clear interannual variations and are believed to be a result of the variation of wind stress associated with El Niño events according to the studies of Xie et al. (2003) and Wang, Fang et al. (2006). Xie et al. (2003) found that the cold filament and mid-summer cooling did not occur in 1998, following the strong 1997/1998 El Niño event. The numerical simulation by Wang, Fang et al. (2006) confirms that the VOC and its associated upwelling vanish in the summer of 1998.

3.2 *Upwelling off the southeast Vietnamese coast*

Associated with the VOC, strong upwelling spreading eastward from the Vietnamese coast can be observed. Wyrtki (1961) found that the sea surface temperature (SST) off the coast of Vietnam in June and July shows a drop of more than 1℃. From the numerical simulation Chao et al. (1996) found that the upwelling begins in August at about 16°N and extends southward until October, and its center can be identified at 150 m. The field hydrographic observations of Fang, Guo et al. (1998) and Fang et al. (2002) show that the upwelling extends to below 300 m depth in the September of 1994. From the observation carried out in July along the coast of Vietnam, the upwelling was also well identified by the shallower isohalines and higher salinity than the nearby areas (Penjan et al., 2001).

The low SST can also be clearly observed from satellite images (Kuo et al., 2000; Xie et al., 2003). Figure 5 displays the climatological mean SST from June to September derived from the SODA [simple ocean data assimilation, see Carton and Giese (2008)] reanalysis. It can be seen that the low SST begins to appear in June in the nearshore area between 11° and 16°N and spreads eastward in July. In August the low SST area further extends eastward to approach the eastern boundary of the SCS, with its center shifting slightly southward. The VOC is a main conveyor that transports the upwelled cold water eastward. The cold water can be further transported southward by the eastern segment of the anticyclonic gyre south of the VOC (Fig. 3b). It is worth noting that the SST in the central and southern SCS (roughly south of 16°N) reaches the highest temperature in late spring (May) rather than in summer. The VOC and its associated upwelling may play an important role in the seasonal evolution of SST and the overlying atmosphere surface temperature in this area.

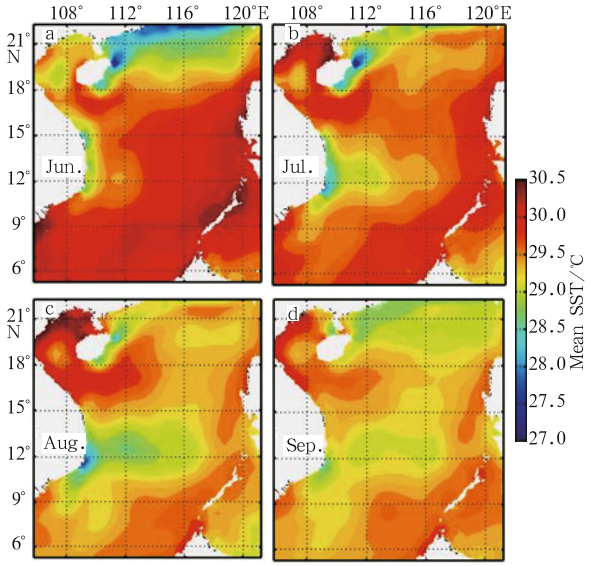

Fig.5. Climatological mean SST for June, July, August and September from SODA reanalysis (averaged over 1987–2008).

In the summers following El Niño events, the upwelling tends to vanish, resulting a basin-wide warming-up of the SCS. A typical warm event occurring in the summer of 1998 was first reported by Wang et al. (2002). Fang et al. (2006) evaluated the correlation between the SCS SST and the El Niño index, and show that the greatest correlation coefficient with El Niño3.4 index appears off the southeast Vietnamese coast (their Fig. 13).

3.3 *Meander and cyclonic gyre north of VOC–A bimodal behavior?*

In summer the anticyclonic gyre south of the VOC is stable and is well recognized (Figs 2b and 3b). Liu et al. (2000) reported that during the cruise conducted in June–July of 1998 an anticyclonic warm gyre at 100 m layer was found off the southeast coast of Vietnam.

The warm gyre covers an even larger area at 700 m layer and extended southwards. At 1 200 m depth, the central SCS and the western are all controlled by the warm gyre. The barotropical models of Li et al. (1994) and Fang et al. (1996) predicted that there also exists a cyclonic gyre off the coast of central Vietnam and to the north of the VOC in July. Based on the hydrographic observation in September 1994, Fang, Guo et al. (1998) speculated that a cyclonic circulation might exist north of the VOC. The cyclonic gyre was also drawn by Fang, Fang et al. (1998) with a dashed arrow (Fig. 3b), indicating possible existence of the structure. Wang, Chen et al. (2006) believed that the southern anticyclonic gyre and the northern cyclonic gyre (they called them eddies) were concomitant features, and called them a dipole structure, which began in June and peaked in August or September. The numerical model of Wang, Fang et al. (2006) reproduced the dipole in August (their Fig. 14f). The dipole has both interdecadal variability (Wang et al., 2010) and interannual variability (Chen, Hou et al., 2012).

However, after scrutinizing the climatological monthly mean SSH maps produced from the SODA reanalysis (Fig. 6), we found that the southern anticyclonic gyre is strong and stable as revealed by the previous studies. The cyclonic gyre north of the VOC cannot be seen in June or July at least in terms of climatological mean. During this period the flow separated from the VOC firstly goes northward, and turns to northwest at about 14°N, and then turns toward northeast, forming a meandering flow to the east of the northward coastal current. This meander becomes stronger and begins to form a cyclonic eddy in later summer (August), and then is replaced by a cyclonic gyre in early fall (September). Meanwhile, the coastal current is reversed from northward to southward. This seems to indicate that a bimodal behavior may occur off the central Vietnamese coast in summer. The cyclonic vorticity associated with the velocity shear on the northern edge of the VOC and the wind stress curl off the central Vietnamese coast is in favor of the formation of a cyclonic gyre, while the southwest monsoon winds are in favor of the formation of a northward current. The relative intensity of these two effects may determine the behavior of the current off the central Vietnamese coast. The above characteristics can also be observed from the climatological monthly mean SSHA maps derived from satellite altimeter measurements. It is worth to mention that the summer SSHA maps usually exaggerate the strength of the northward western boundary current. This is because the summer SSHA is the difference between summer SSH and annual mean SSH, while the latter is dominated by the winter circulation. Therefore, the summer SSHA, mathematically, is determined mainly by the summer SSH and the winter SSH. That is, the summer SSHA cannot well reflect the summer circulation. Instead, it usually overestimates the strength of the summer western boundary current due to the strong winter western boundary current (Li et al., 2000). This is the reason why we prefer to use SODA SSH results rather than the altimeter SSHA product in the above analysis.

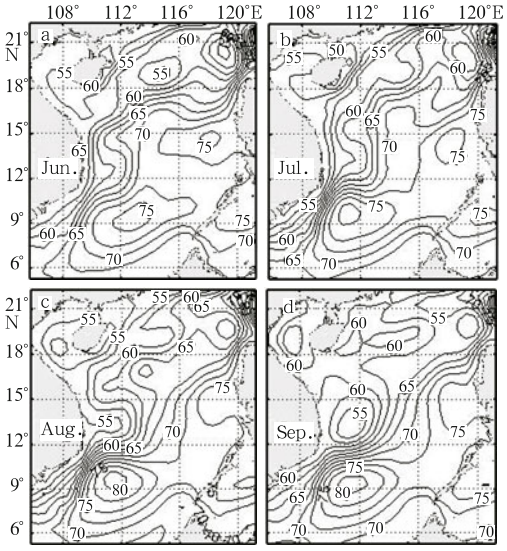

Fig.6. Climatological mean SSH (in cm) for June, July, August and September from SODA reanalysis (averaged over 1987–2008).

In the summers following El Niño events, the VOC generally diminishes and the structures mentioned above also vanish, leaving a simple northward coastal current along the southern and central Vietnamese coasts, as seen from the model result of Wang, Chen et al. (2006, their Fig. 14d) for the summer of 1998.

There may be two reasons for Li et al. (1994) and Fang et al. (1996) to obtain the northern cyclonic gyre in July. One possible reason is that the response of their barotropic models may be too faster with respect to the baroclinic response in the real ocean. This speculation is supported by the fact that the July circulation pattern obtained from their barotropic models resembles the September pattern from the SODA reanalysis. The other reason is that their models are vertically integrated models, therefore the currents ob-

tained from their models actually include both the surface and subsurface flows, and the latter may have opposite directions to the former.

The summer western boundary current in the southern SCS can reach a depth of about 400 m as observed from the hydrographic survey in September 1994 (Fang, Guo et al., 1998b). The ADCP current observation at 11°16′N, 110°46′E in May 2002 by Du et al. (2004) shows that the flows are persistently northward from the surface down to 540 m (Note that the observational period is in May, when the northward western boundary current has just established and the VOC has not formed yet). Figure 7 shows the climatological mean zonal velocities across the meridional-vertical section along 111.25°E for June through September, obtained from the SODA reanalysis. It can be seen that the currents can reach the depths of 300 to 400 m.

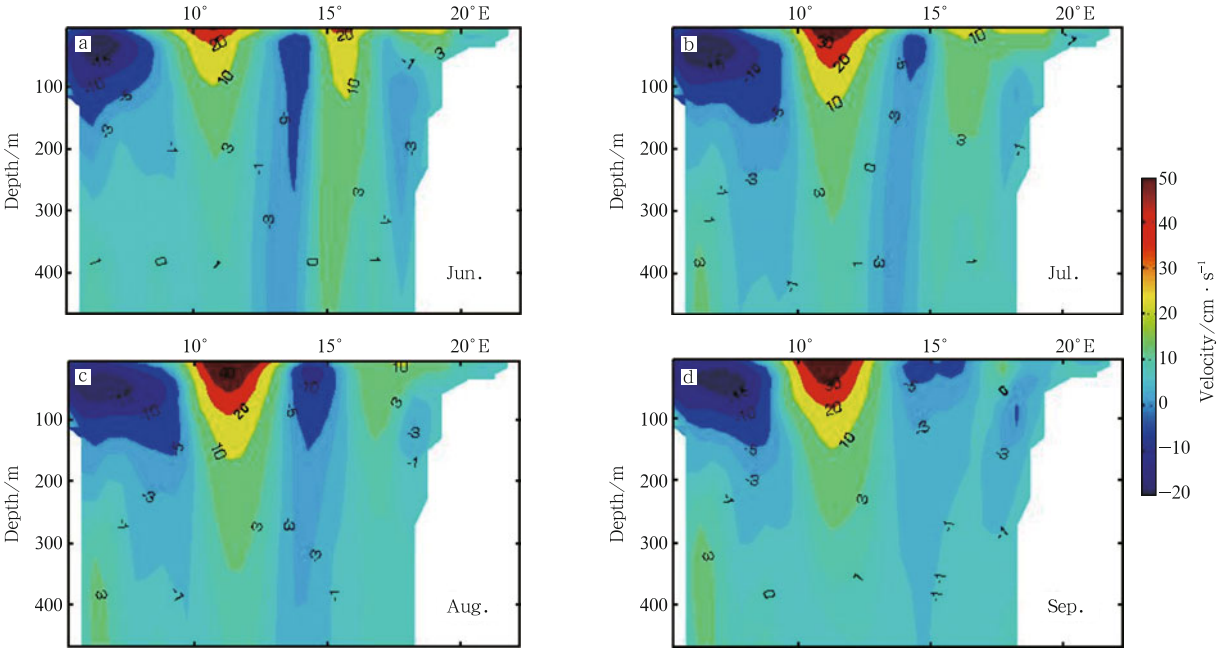

Fig.7. Climatological mean zonal velocity (in cm/s) across the meridional-vertical section along 111.25°E for June, July, August and September from SODA reanalysis (averaged over 1987–2008). Positive values represent eastward velocity.

It is likely that the northward coastal current and the northward meandering current off the central Vietnamese coast are mainly upper layer features. Beneath these features there is possibly a southward subsurface current, which originates from the area near the South China continental slope (see the next subsection). This subsurface current might join the VOC and form a subsurface cyclonic gyre off the central Vietnamese coast in July or even in June. The in situ observation is necessary in verifying this hypothesis.

3.4 *Summer SCS Warm Current and a southwestward subsurface current*

The current southeast of Hainan Island in summer is northeastward. This can be evidenced by the upwelling along the east coast of the island. The surface flows on the South China shelf are generally northeastward and will eventually enter the Taiwan Strait. Following Guan (see Kwan, 1978), this current is called the summer SCS Warm Current (Fang, Fang et al., 1998).

The current structure near the South China continental slope is still not well understood yet. The earliest works of Dale (1956) and Wyrtki (1961) indicate that the summer currents in this area are toward the northeast (Figs 1b and 2b). Most three-dimensional numerical models also give northeastward currents in summer months (from late May to August), as seen in the results of SODA reanalysis (Fig. 6). Products based on altimeter measurements also indicate northeastward currents in summer (e.g., Li et al., 2000). On the contrary, however, based on the

hydrographic observation Qiu et al. (1984) found that the currents near the Dongsha Islands are southwestward, and proposed that these currents originated from the Kuroshio. Based on current observations Huang et al. (1997) also found the southwestward currents along the continental slope north of the Dongsha Islands. Su (2004) suggested that the western boundary current near the Dongsha Islands are southwestward in all seasons, and called it the Dongsha Current. Driven by the southwesterly monsoon the summer surface currents in the Luzon Strait contain an eastward component, as can be verified by the fact that no satellite-tracked drifters in the Pacific can enter the SCS in all summer months. Fang et al. (2009) found that the outward volume transport through the Taiwan Strait and the upper layer of the Luzon Strait exceeds the inward volume transport through the Karimata Strait, and proposed that a subsurface inflow across the Luzon Strait from the Pacific to the SCS is required in summer to balance the water loss in the upper layer of the SCS. It is quite possible that this subsurface inflow continues to progress southwestward along the South China continental slope. The model result of Wang, Chen et al. (2006, their Fig. 3) shows that the currents at 100 m depth are southwestward in all seasons and can reach the area off the central Vietnamese coast. This subsurface current may extend down to intermediate layer according to the P-vector computation of Chu and Li (2000, their Fig. 9). It seems that this southwestward current generally appears as a subsurface current in summer. It might be able to ascend to the surface in some areas as suggested by Qiu et al. (1984), but further observational evidences are needed.

4 Concluding remarks

It is generally believed that the SCSwbc is characterized by a southward (or southwestward) flow in winter and a northward (or northeastward) flow in summer as shown by Dale (1956) and Wyrtki (1961). The investigations in the last three decades have revealed abundant structures of this current. We propose the following as the most distinguished features.

(1) From October to December the SCSwbc runs southwestward along the South China continental shelf and slope and turns southward along the Vietnamese coast. When it reaches the Sunda Shelf, one part of it continues to flow towards the Java Sea through the Karimata Strait, and the other part turns eastward to form the a cyclonic gyre.

(2) In January and February, the SCSwbc appears to consist of two segments, which are separated by a sea-surface height ridge extending eastward roughly along 13°N from the Vietnam coast. These two segments appear to be continuous in the surface layer due to Ekman drift, while their geostrophic components may be blocked by the ridge.

(3) The SCSwbc in summer can be roughly divided into three segments. The southern segment is from the Karimata Strait to the turning point of the Vietnamese coastline at about 11°N. It then turns to the east to form an offshore current called the Vietnam Offshore Current (VOC). Associated with the VOC, strong upwelling occurs near the southeast Vietnamese coast and spreads eastward, which pumps deep cold water upward to cool the sea surface and the overlying atmosphere.

(4) The middle segment off the central Vietnamese coast may have a bimodal behavior: a northward coastal current and a meandering current in early summer (June–July), and a cyclonic gyre in late summer and early fall (August–September).

(5) The northern segment is featured by the summer SCS Warm Current on the South China shelf and a southwestward subsurface current along the continental slope.

The general circulation in the SCS has great similarity to that in the great open oceans but is much more variable than the latter due to its relative smaller spatial scale and the more variable forcing of monsoon (Wang et al., 2009). Further in situ observations are still required to verify the known features and to reveal undiscovered features. In particular, long-term measurements are required to quantitatively estimate the volume and property transports of each segment of the current.

References

Bao Lifeng, Lu Yang, Wang Yong, et al. 2005. Seasonal variation of upper ocean circulation over the South China Sea from satellite altimetry data of many years. Chin J Geophys (in Chinese), 48(3): 543–550

Cai Shuqun, He Yinghui. 2010. Association of the Sulu Sea surface circulation with the South China Sea. J Mar Syst, 81: 335–340

Cai Shuqun, Long Xiaomin, Wang Shengan. 2007. A model study of the summer Southeast Vietnam Offshore Current in the southern South China Sea. Cont Shelf Res, 27: 2357–2372

Carton A C, Giese B S. 2008. A reanalysis of ocean climate using simple ocean data assimilation (SODA). Mon Weather Rev, 136: 2999–3017

Chao Jiping, Feng Licheng, Wang Dongxiao, et al. 2006. Asymptotic theory of the wind-driven boundary jet's stability. Chin J Geophys (in Chinese), 49(3): 642–649

Chao Shenn-Yu, Shaw Ping-Tung, Wang Joe. 1995. Wind relaxation as a possible cause of the South China Sea warm current. J Oceanogr, 51: 111–132

Chao Shenn-Yu, Shaw Ping-Tung, Wu S Y. 1996. Deep water ventilation in the South China Sea. Deep-Sea Res, 43: 445–466

Chen Gengxin, Hou Yijun, Zhang Qilong, et al. 2012. The eddy pair off eastern Vietnam: interannual variability and impact on themohaline structure. Cont Shelf Res, 30: 715–723

Chen Weifang, Liu Qian, Huh Chih-An, et al. 2010. Signature of the Mekong River plume in the western South China Sea revealed by radium isotopes. J Geophys Res, 115: C12002

Chern Ching-Sheng, Wang Joe. 2003. Numerical study of the upper-layer circulation in the South China Sea. J Oceanogr, 59: 11–24

Chu P C, Chen Yuchun, Lu Shihua. 1998. Wind-driven South China Sea deep basin warm-core/cool-core eddies. J Oceanogr, 54: 347–360

Chu P C, Edmons N L, Fan Chenwu. 1999. Dynamical mechanisms for the South China Sea seasonal circulation and thermohaline variabilities. J Phys Oceanogr, 29: 2971–2991

Chu P C, Li Rongfeng. 2000. South China Sea isopycnal-surface circulation. J Phys Oceanogr, 30: 2419–2438

Dale W L. 1956. Wind and drift currents in the South China Sea. The Malaysian J Trop Geogr, 8: 1–31

Dippner J W, Nguyen K V, Hein H, et al. 2007. Monsoon-induced upwelling off the Vietnamese coast. Ocean Dyn, 57: 46–62

Du Yan, Wang Dongxiao, Chen Rongyu, et al. 2004. Vertical structure of ADCP observed current in the western boundary of the South China Sea. The Ocean Engineering (in Chinese), 22(2): 31–38

Fang Guohong, Chen Haiying, Wei Zexun, et al. 2006. Trends and interannual variability of the South China Sea surface winds, surface height, and surface temperature in the recent decade. J Geophys Res, 111: C11S16

Fang Wendong, Guo Zhongxin, Huang Yuting. 1998. Observational study of the circulation in the southern South China Sea. Chin Sci Bull, 43: 898–905

Fang Wendong, Fang Guohong. 1998. The recent progress in the study of the southern South China Sea circulation. Advance in Earth Sciences (in Chinese), 13(2): 166–172

Fang Guohong, Fang Wendong, Fang Yue, et al. 1998. A survey of studies on the South China Sea upper ocean circulation. Acta Oceanographica Taiwanica, 37: 1–16

Fang Wendong, Guo Junjian, Shi Ping, et al. 2006. Low frequency variability of South China Sea surface circulation from 11 years of satellite altimeter data. Geophys Res Lett, 33: L22612, doi: 10.1029/2006GL027431

Fang Wendong, Fang Guohong, Shi Ping, et al. 2002. Seasonal structures of upper layer circulation in the southern South China Sea from in situ observations. J Geophys Res, 107(C11): 3202, doi:10.1029/2002JC001343

Fang Yue, Fang Guo-hong, Yu Ke-jun. 1996. ADI barotropic ocean model for simulation of Kuroshio intrusion into China southeastern waters. Chin J Oceano Limno, 14: 357–366

Fang Guohong, Susanto R D, Soesilo I, et al. 2005. A note on the South China Sea shallow interocean circulation. Adv Atmos Sci, 22: 946–954

Fang Guohong, Susanto R D, Wirasantosa S, et al. 2010. Volume, heat, and freshwater transports from the South China Sea to Indonesian seas in the boreal winter of 2007–2008. J Geophys Res, 115: C12020, doi:10.1029/2010JC006225

Fang Guohong, Wang Yonggang, Wei Zexun, et al. 2009. Interocean circulation and heat and freshwater budgets of the South China Sea based on a numerical model. Dyn Atmos Oceans, 47(1–3): 55–72

Guo Zhongxin, Yang Tianhong, Qiu Dezhong. 1985. The South China Sea Warm Current and a southwestward current on its right-side in winter. Tropical Oceanology (in Chinese), 4(1): 1–8

He Zhigang, Sui Dandan. 2010. Remote sensing and validation of the South China Sea western boundary current in December 2003, 2004 and 2005. Proceeding of 2010 Second IITA International Conference on Geoscience and Remote Sensing, Qingdao, 515–518. IEEE, doi: 10.1109/IITA-GRS.2010.5602670

Ho Chung-Ru, Kuo Nan-Jung, Zheng Quanan, et al. 2000. Dynamically active areas in the South China Sea detected from TOPEX/POSEIDON satellite altimeter data. Remote Sens Environ, 71: 320–328

Hu Jianyu, Kawamura H, Hong Huasheng, et al. 2000. A review on the currents in the South China Sea: Seasonal circulation, South China Warm Current and Kuroshio intrusion. J Oceanogr, 56: 617–624

Huang Qizhou, Wang Wenzhi, Fu Suncheng, et al. 1997. A westward current that flows through the north of the Dongsha Islands in summer. Tropical Oceanology, 16(2): 58–66

Kuo Nan-Jun, Zheng Quanan, Ho Chung-Ru. 2000. Satellite observation of upwelling along the western coast of the South China Sea. Remote Sensing of Environment, 74: 463–470

Kwan Pingshien. 1978. The warm current in the South China SeaCA current flowing against the wind in winter in the open sea off Guangdong Province. Oceanologia et Limnologia Sinica (in Chinese), 9(2): 117–127

Li Rongfeng, Huang Qizhou, Wang Wenzhi. 1994. Numerical simulation of South China Sea upper layer currents. Acta Oceanologica Sinica (in Chinese), 16(4): 13–22

Li Li, Wu Lisheng, Guo Xiaogang. 2000. Seasonal circulation in the South China Sea–A TOPEX/Poseidon satellite altimetry study. Acta Oceanologica Sinica (in Chinese), 22(6): 13–26

Liu Zhengyu, Yang Haijun, Liu Qinyu. 2001. Regional dynamics of seasonal variability in the South China Sea. J Phys Oceanogr, 31: 272–284

Liu Yonggang, Yuan Yaochu, Su Jilan, et al. 2000. South China Sea summer circulation in 1998. Chin Sci Bull (in Chinese), 45(12): 1252–1259

Metzger E J, Hurlburt H E. 1996. Coupled dynamics of the South China Sea, the Sulu Sea, and the Pacific Ocean. J Geophys Res, 101: 12331–12352

Penjan R, Siriporn P, Natinee S, et al. 2001. Temperature, salinity, dissolved oxygen and water masses of Vietnamese waters. Proceeding of the SEAFDEC Seminar on Fisheries resources in the South China Sea area IV, Vietnamese Waters. Thailand: Southeast Asian Fisheries Development Center, 346–355

Qiu Dezhong, Yang Tianhong, Guo Zhongxin, 1984. A west-flowing current in the northern part of the South China Sea in summer. Tropical Oceanology (in Chinese), 3(4): 65–73

Qu Tangdong, Kim Y Y, Yaremchuk M, et al. 2004. Can Luzon Strait transport play a role in conveying the impact of ENSO to the South China Sea? J Climate, 17: 3644–3656

Rong Zengrui, Liu Yuguang, Zong Haibo, et al. 2007. Interannual sea level variability in the South China Sea and its response to ENSO. Global and Planetary Change, 55: 257–272

Shaw Ping-Tung, Chao Shenn-Yu. 1994. Surface circulation in the South China Sea. Deep-Sea Res: I, 41: 1663–1683

Shaw Ping-Tung, Chao Shenn-Yu, Fu Lee-Lueng. 1998. Sea surface height variations in the South China Sea from satellite altimetry. Oceanologica Acta, 22: 1–17

Su Jilan. 2004. Overview of the South China Sea circulation and its influence on the coastal physical oceanography outside the Pearl River Estuary. Cont Shelf Res, 24: 1745–1760

Takano K, Harashima A, Nnmba T. 1998. A numerical simulation of the circulation in the South China Sea–Preliminary results. Acta Oceanographica Taiwanica, 37: 165–186

Tangang F T, Xia Changshui, Qiao Fangli. 2011. Seasonal circulations in the Malay Peninsula eastern continental shelf from a wave-tide-circulation coupled model. Ocean Dyn, 61: 1317–1328

Wang Yonggang, Fang Guohong, Wei Zexun, et al. 2006. Interannual variation of the South China Sea circulation and its relation to El Niño, as seen from a variable grid global ocean model. J Geophys Res, 111: C11S14

Wang Bin, Huang Fei, Wu Zhiwei, et al. 2009. Multiscale climate variability of the South China Sea monsoon: a review. Dyn Atmos Oceans, 47: 15–37

Wang Liping, Koblinsky C J, Howden S. 2000. Mesoscale variability in the South China Sea from the TOPEX/Poseidon altimetry data. Deep-Sea Res: I, 47: 681–708

Wang Dongxiao, Xie Qiang, Du Yan et al. 2002. The 1997–1998 warm event in the South China Sea. Chin Sci Bull, 47(14): 1221–1227

Wang Guihua, Chen Dake, Su Jilan. 2006. Generation and life cycle of the dipole in the South China Sea summer circulation. J Geophys Res, 111: C06002, doi:10.1029/2005JC003314

Wang Guihua, Wang Chunzai, Huang Ruixin. 2010. Interdecadal variability of the eastward current in the South China Sea associated with the summer Asian monsoon. J Climate, 23: 6115–6123

Wang Chunzai, Wang Weiqiang, Wang Dongxiao, et al. 2006. Interannual variability of the South China Sea associated with El Niño. J Geophys Res, 111: C03023

Wyrtki K. 1961. Physical oceanography of the southeast Asian waters. NAGA Report 2. San Diego: eScholarship Repository, Scripps Institute of Oceanography, University of California

Xie Shang-Ping, Xie Qiang, Wang Dongxiao. 2003. Summer upwelling in the South China Sea and its role in regional climate variations. J Geophys Res, 108(C8): 3261

Zhou Hui, Yuan Dongliang, Li Ruixiang, et al. 2010. The western South China Sea currents from measurements by Argo profiling floats during October to December 2007. Chin J Oceano Limno, 28: 398–406